THEORETICAL STUDY OF PHYSIOCHEMICAL PROPERTIES OF INSULIN-LIKE GROWTH FACTOR 1

A Ilkhani
Department of Chemistry, Yazd Branch, Islamic Azad University, Yazd, Iran.
Email: ilkhaniali@yahoo.com

ABSTRACT

The computational approach to studying structural changes in a wide range of physical and biological problems, the empirical force fields, have great difficulty in simulating folding of Insulin-like Growth Factor 1 (IGF-1). In an effort to understand the conformational preferences that may be attributed to stereoelectronic effects, a number of computational studies were carried out. Monte Carlo, Molecular Dynamics and Langevin simulation methods by MM+, AMBER and OPLS force fields of calculations have been performed on IGF-1 as growth factors. The parameters of a minimized structure of IGF-1, calculated potential energy for important dihedral angles and the effect of temperature on the geometry of optimized structure have been calculated. Prediction simulation methods of lattice model have mostly used different temperatures at gas and water media but we have seen that in simulation approaches, scaling up the interaction energy has a similar effect to lowering temperature. This study has demonstrated that the simple model, which includes an approximate average solvent effect, can simulate the qualitative feature of the IGF-1. The results of this investigation can be tested computationally to see whether the solvent effect can study the aspect of structural changes resulting from the average solvent effect. The main research problem was to find the dynamics of biomolecular structure and an appropriate effective stabilized energy.

Keywords: IGF-1, AMBER, MM+, OPLS, MC, MD, LD.

INTRODUCTION

Our research group uses structural bioinformatics methods to study the structure, function and dynamics of biomolecules. Our goal is to understand and obtain structural formation of biomolecules and the mechanism of their association. The function of proteins or nucleic acids depends on its three-dimensional structure and conformational dynamics. We employ the molecular dynamics simulation method as the main tool to study conformational dynamics of biomolecules. This approach allows following dynamic molecular processes at high resolution in space and time. It is also possible to study the thermodynamics and energetic of structure formation and association. Our research in general was not restricted to a single biomolecular system.

Insulin-like growth factor (IGF-1), also known as somatomedin C, mediates the growth promoting activity of the growth hormone. IGF-1 is an autocrine regulator of cell proliferation, paracrine growth and survival factor for mammalian embryo development (Emmitte *et al.* 2009). Recent NMR studies have revealed that IGF-I has three α-helical regions surrounding a hydrophobic core (Laajok *et al.* 2000).

The over expression or auto activation of the insulin-like growth factor-1 receptor (IGF-1R) tyrosine kinase has been associated with various cancers. Insulin-like growth factor (IGF-1) is an anti-apoptosis factor of multiple cell types, and the anti-apoptotic effects are mediated through mitochondrial and cytochrome-c pathway (Li *et al.* 2003).

Development of faster computers that are within the reach of the widest scientific community as well as efficient computational methods allows investigating systems between 50–100 atoms in the frame of quantum mechanics and up to 50,000 atoms with molecular dynamics. Since the models have become increasingly realistic, direct comparison with experimental data becomes possible (Náray-Szabó and Berenteb 2003). In addition to identification, docking techniques are increasingly used to support lead optimization efforts (Kitchen *et al.* 2004).

Recently, constant temperature molecular simulations of peptide folding have been reported using implicit and explicit solvent models (Sung and Wu 1997, Daura *et al.* 1998). However, several computer simulations have demonstrated a strong coupling between hydrophobicity, solute-solvent dispersion attractions and electrostatics. For example, simulations of explicit water between plate like solutes revealed that hydrophobic attraction and dewetting phenomena are strongly sensitive to the nature of solute-solvent dispersion interactions (Dzubiell *et al.* 2006).

The competing effects of the solvent, such as the van der Waals (VDW) attraction and hydrogen bonding between the protein and solvent, reduce the strength of the interactions and consequently reduce the energy barrier related to the multiple minima problem (Ozkan *et al.* 2004). In solution, the intramolecular VDW interactions of a protein molecule are balanced by the intermolecular VDW interactions with solvent molecules. The possible difference, between the protein intramolecular VDW attraction and that with water may be included in the hydrophobic interaction energy (Ozkan *et al.* 2004). Kurochkina and Lee have shown that the pair wise sum of the buried surface area is linearly related to the true buried area (Sung 1999).

Since the specific interactions between the residues and solvent play an important role in the stability of the native structure, it is useful to carry out such simulations at atomistic detail. This comes with the problem of timescale of folding/unfolding that is several orders of magnitude larger than those currently attainable by MD simulations (Ozkan *et al.* 2004). Water plays a crucial role for the stability, dynamics and function of proteins. For this reason Molecular Dynamics (MD), Monte Carlo (MC) and Langevin Dynamics (LD) simulations must account for the effects that this solvent has, both on protein structure and on protein dynamics (Hamaneh and Buck 2007).

The aim of the present work was to describe and characterize the molecular structure, vibrational properties of IGF-1. The structures of a coordination compound modeling the IGF-1 computationally is described. Thus, it is worthwhile to collect information on the structures by the means of computational chemistry as well.

METHOD

The crystal structures of proteins were from the Brookhaven Protein Data Bank. The structure of protein IGF-1 was selected from the Protein Data Bank (PDB code 1B9G). These studies provided insights into the steric, electrostatic, hydrophobic, and hydrogen bonding properties and other structural features influencing the IGF-1. In vacuum the system was simulated using Monte Carlo, Molecular dynamics and Langevin dynamics with 100 ps step and without any constraints. Temperature was kept constant at 300 K. In water, the simulated system was placed in a box (3 x 3 x 3 nm) containing one molecule of solute and 884 TIP3P water molecules (Fig. 1). The system was simulated using Newtonian dynamics with 100 ps step and no constraints applied to the solute. Monte

Carlo simulations are based on pair-wise additive potentials of the form described by Tafazzoli and Khanlarkhani (2007). In concepts and algorithms of classical MD simulations the atoms of a biopolymer move according to the Newtonian equations of motion (Berendsen 1990). The electrostatic potential energy is represented as a pairwise summation of coulombic interactions (Phillips *et al.* 2005). In equation, *N* is the number of atoms in molecules A and B, respectively, and *q* the charge on each atom (Kitchen *et al.* 2004). We can consider an effective Hamiltonian operator as constructed for a molecule in a given geometry of it and the solvent where H_0 is the Hamiltonian in gas phase (the unperturbed Hamiltonian), V_{elec} is the perturbation from the permanent charge distribution of water, represented as a set of point-charges, V_{ind} is the perturbation from the induced dipoles in the solvent and $V_{non-elec}$ is a non-electrostatic perturbation, which models the effect of the anti-symmetry between the solute and solvent (Hermida-Ramón *et al.* 2009).

Using Langevin dynamics, you can model solvent effects and study the dynamical behavior of a molecular system in a liquid environment. These simulations can be much faster than molecular dynamics. These simulations can be used to study the same kinds of problems as molecular dynamics, i.e., time dependent properties of solvated systems at non-zero temperatures. Because of the implicit treatment of the solvent, this method is particularly well-suited for studying large molecules in solution.

Langevin dynamics simulates the effect of molecular collisions and the resulting dissipation of energy that occur in real solvents, without explicitly including solvent molecules. This is accomplished by adding a random force and a frictional force to each atom at each time step. Mathematically, this is expressed by the Langevin equation of motion (Berendsen 1990). Molecular mechanics (MM) force fields rely on the combination of Coulomb and Lennard–Jones interactions to describe all nonbonded interactions (Ponder and Case 2003). Even though the functional form of the potential energy is quite simple, it depends on a large number of empirical parameters, which must be obtained from ab initio electronic structure calculations on small molecules and/or experimental data.

Because each new term in the MM potential function requires additional empirical parameters, it is quite appealing to keep the functional form of the potential function as simple as possible. While most widely used current force fields such as AMBER, OPLS do not employ explicit hydrogen bonding terms, this was not always the case (MacKerrell *et al.* 1998, Hagler and Lifson 1974, Cornell *et al.* 1995, Jorgensen *et al.* 1996, Weiner *et al.* 1984).

RESULTS AND DISCUSSION

The complex was solvated by added water molecules. The systems were first energy minimized steps with the conjugate gradient algorithm. Then, the position-restrained MC, MD and LD simulation were run 100 ps. Afterwards, 1 ps simulations were carried out at a time step of 100 ps (Fig. 1). Several simulations were carried out, as listed in Table 1. MC, MD and LD simulations of the IGF-1 were performed with the HyperChem7.0 program (HyperChem 2001). The geometries, and the interaction energies, bonds, angles, stretch-bends, electrostatic and the VDW Interactions were carried out in solution and in gas phase (Table 1 and Fig. 2).

In solution, the intramolecular VDW interactions of a protein molecule are balanced by the intermolecular VDW interactions with solvent molecules. Thus, when solvent molecules are not explicitly included, the intramolecular VDW

interactions must be adjusted accordingly. The longer-range attractive VDW interactions provide a nearly uniform background potential (Chandler *et al.* 1983), and therefore can serve as the reference for the VDW energy calculation (McCammon *et al.* 1980).

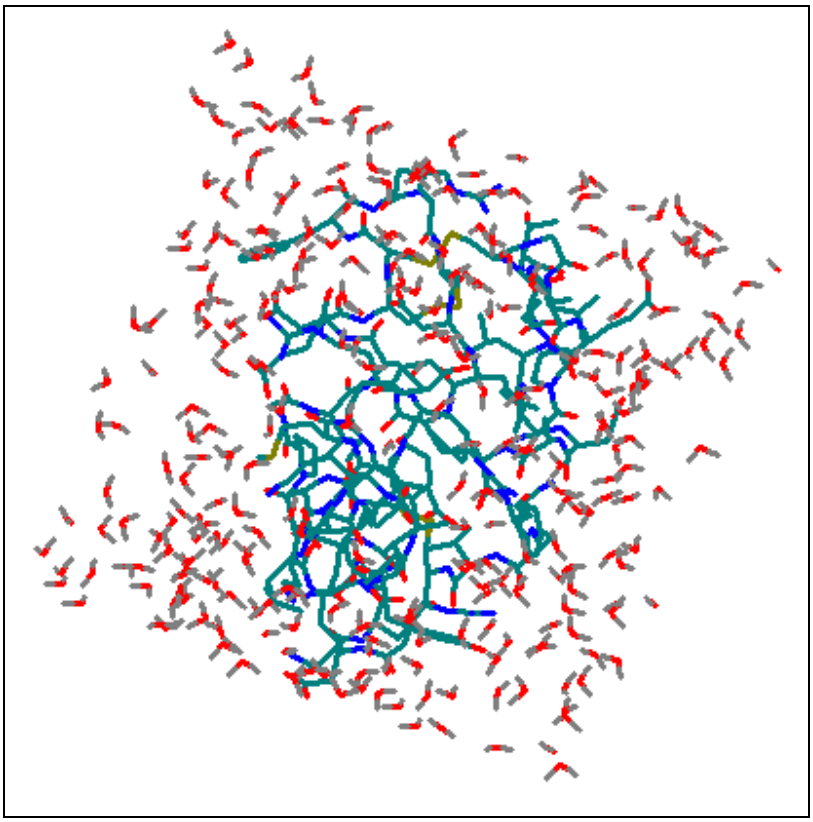

Figure 1: Schematic representation of structural model of IGF-1R in water (884 TIP3P water molecules).

The following text describes methods for generating and evaluating representative molecular conformations, particularly for peptides and small proteins, based on Molecular Mechanics energy functions. On the other hand, Molecular Mechanics describes molecules as atoms linked with springs (harmonic bond stretches and bond angle wagging), each atom having finite volume and relatively sharp boundaries ("6-12" hard spheres potentials), with sinusoidal torsional energies. The force field for a typical protein can be given as a sum of the various components including bond stretching and bending, torsional potentials, and non-bonded interactions.

Table 1: Calculated variables at 300 K Temperature for IGF-1 at MM+, AMBER and OPLS.

	GEOMETRY					
environment	**Force Field**	**Bond**	**Angle**	**Dihedral**	**Energy**	**Gradient**
gas	**MM+**	174.408	2003.05	187.056	2186.66284	0.099337
	AMBER	11.0393	67.3022	200.754	23.23151	0.099951
	OPLS	2.53763	47.7753	48.4863	-202.51639	0.098917
water	**MM+**	202.777	2037.84	43.0804	-130.11968	0.095515
	AMBER	175.662	2019.97	212.994	270.345123	0.084089
	OPLS	175.662	2019.97	212.994	270.345123	0.084089

	MC	**MD**			**LD**		
environment	**Potential**	**Potential**	**Kinetic**	**Total Energy**	**Potential**	**Kinetic**	**Total Energy**
gas	547.949	2456.24	386.747	2842.99	354.473	388.198	742.671
	2798.14	348.117	393.388	741.505	2481.28	394.672	2875.95
	349.788	138.21	390.617	528.827	131.714	391.538	523.253
water	2217.07	6677.62	9695.98	16373.6	672.07	1562	2300.2
	160.52	733.188	1608.57	2341.76	746.05	1596	2342.05
	1367.75	686.563	1826.73	2513.3	641.945	1871.01	2512.95

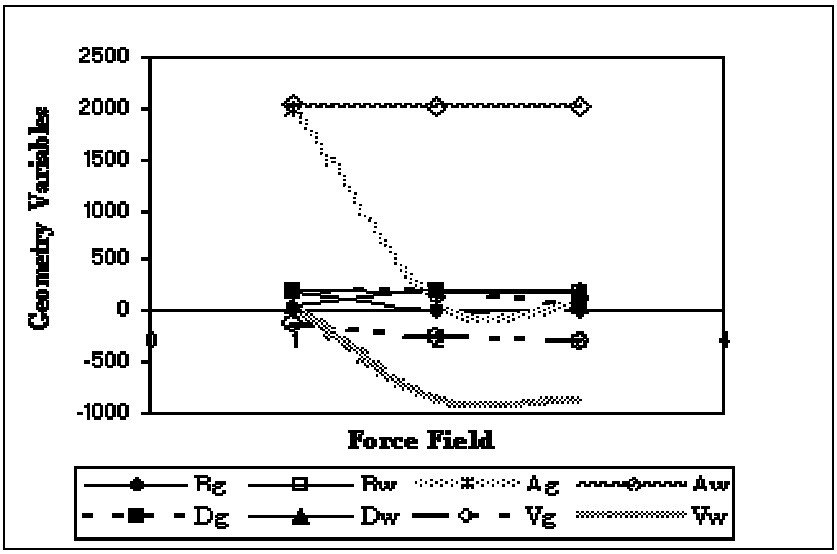

Figure 2: Geometry optimized variables of Bond length (B),Bond Angle (A) and Dihedral Angle (D) in gas and water media at 300K.

In this paper, we have used Monte Carlo methods to study IGF-1 in the bulk and in confined environments. Results are presented in Table 1 effects on the specific media of the structure. The potential energy was for the growth factor (IGF-1) with water during the MC simulation is shown in Fig. 3. Molecular dynamics simulations were carried out on the two systems, gas and solvent IGF-1 molecule. All simulations were carried out at constant temperature. All simulations were performed at 300 K. Each solvent system was immersed in a periodic water box, and the structures of water molecules were maintained. A 100 ps time step was used in all the simulations. The potential energy, represented through the MD "force field," is the most crucial part of the simulation since it must faithfully represent the interaction between atoms yet be cast in the form of a simple mathematical function that can be calculated quickly. Molecular dynamic simulations have been widely used to obtain the 'real' bioactive conformation when the crystal structure of protein–ligand complex is unavailable. So, in order to obtain the 'real' stabilized bioactive compound was used for molecular dynamics simulations. MD simulation is suitable for obtaining the elastic properties of a system the size of ours.

The system was well equilibrated and 500 ps in the range of the MD equilibration were selected for further processing analysis. After equilibration, the MD simulation was very stable, and in order to compare the difference between the relation coefficients (R^2 = 0.8173 in gas and R^2 = 0.7558 in water) as we have shown in Fig. 3, respectively. The theoretically possible stable conformers of free molecule were searched by means of a molecular dynamics calculation performed in a temperature interval from 0 to 500 K; for example, the iterative calculation with time step of ''100 ps", carried out by utilizing the software ''Chem3D" and the experimental X-ray geometrical data reported for IGF-1 in crystalline structure were used as input

geometrical data. At the next step, the appropriate ones carefully selected from the structures obtained throughout this calculation were optimized using MM+, AMBER, and OPLS force field parameters included into the same software. In this paper, a comprehensive conformational search on free molecule was carried out. The obtained results have demonstrated that the free molecule has a very flexible macro-cyclic structure. On the basis of the theoretical results obtained for the determined most stable, the dependencies of the geometrical and force constants parameters of the free molecule to its conformational structure were discussed.

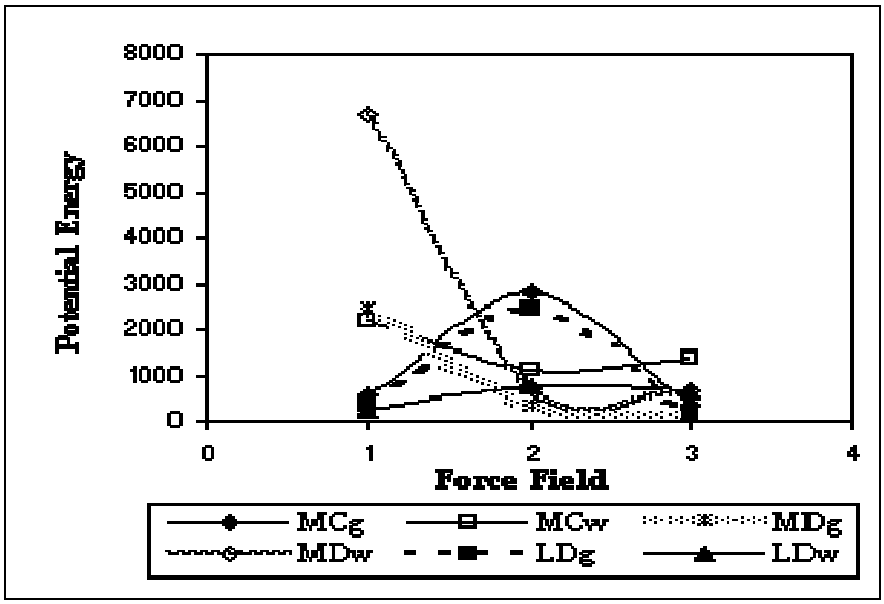

Figure 3: The potential energy(kcal/mol) via time (ps) during Molecular Dynamic (MD) simulation at 300K in gas (R2=0.8173) and water (R2=0.7558) environments to a stabilized structure of IGF-1.

Furthermore, we have used MD and LD methods to study protein in the bulk and in confined environments. The structures obtained throughout this calculation were optimized using MM+, AMBER, and OPLS force field parameters. Also, all these approaches were included discrete particles moving in a defined energy landscape according to Langevin dynamics (LD). These results have shown that the force field of AMBER has convenient relation in all the simulation methods and various media (Fig. 3). From the simulations we have shown that the kinetic temperature of the system is properly bounded around the prescribed equilibrium temperature. The length of each simulation was 100 ps. We have measured the relative drift of molecular temperature, denoted by ΔT in percent, with respect to mean temperature, T in Kelvin. In the simulation of the small water system the temperatures of 295, 297, 299, 301, 303 and 305 K were used (Karplus and Petsko 1990).

These methods, which rely upon uniform sampling of energy space, can yield thermodynamic data over the entire temperature range of interest and have been shown to overcome large free energy barriers. We have reported findings for six

different temperatures of various sizes and topologies. Results presented in table 2 have indicated potential energies of IGF-1 at various temperatures.

For certain confining environments, individual proteins do exhibit power-law dependence, but the relationship is different for each molecule. In other cases, the increase in stability upon confinement interestingly demonstrates nonmonotonic behavior. Several molecular dynamics simulations could be performed over a wide range of temperature, and the data could be combined using a weighted histogram approach (Weiner *et al.* 1984); however, the statistical error associated with the tails of the sampled distributions is usually large and can propagate when data from simulations at different temperatures are merged.

Potential energies for the three force fields of MM+, AMBER and OPLS at Monte Carlo simulation were compared in Fig. 4.The average energies are in good agreement within the simulation accuracy. As expected, AMBER demonstrates much smoother energy profiles than the other two simulation methods due to higher-order energy conservation in the modified Hamiltonian (Fig 4.a). The magnitudes of energy fluctuations in both MM+ and OPLS approaches are significantly smaller than the other (Fig 4.b, c). The sampling results of step-size of MD and LD methods are presented in Figs. 5 and 6, respectively. Observed data are almost identical for both choices of the MD simulation length, which suggests that the MD simulation have affected much more the acceptance rate at least for this particular model than MC and LD approaches. This potential does not have any terms describing angular dependencies of hydrogen bonds and is similar to the 10–12 hydrogen bonding potential originally proposed by (McGuire *et al.* 1972). They found that hydrogen bonding energies were represented adequately by a sum of Lennard–Jones and electrostatic interactions plus the 10–12 hydrogen bonding term with empirical constants adjusted according to the hydrogen bond type.

Because the functional form of such a hydrogen bonding term was very close to the Lennard–Jones component of the force field, the second-generation AMBER force field omitted it altogether (Cornell *et al.* 1995), relying instead on the combination of Lennard–Jones and Coulomb interactions to model hydrogen bonded complexes, thus the data of this force field in three simulation methods has shown the changes of potential energy via time at various temperatures much better than MM+ and OPLS force fields (Fig. 4a, Fig. 5a, Fig. 6a). Similarly, the widely used OPLS force field does not contain an explicit hydrogen bonding term: the emphasis of OPLS parameterization is on reproducing thermodynamic properties of organic liquids such as enthalpies of vaporization, densities, and free energies of hydration (Jorgensen *et al.* 1996, Jorgensen and Tirado-Rives 1988) (Figs. 4b, 5b and 6b). Because each new term in the MM+ potential function requires additional empirical parameters, it is quite appealing to keep the functional form of the potential function as simple as possible (Figs. 4c, 5c and 6c). The effect of confinement on the thermodynamic properties of several statement proteins was investigated by performing simulations over a large range of temperatures. We have computed the transition temperature for the IGF-1 molecule. The results are summarized in Table 1 for 300 K in gas or solvent and in Table 2 for 295, 297, 299, 301, 303 and 305 K temperatures. Figures have shown the function of the reduced temperature. Low reduced temperatures promote complex structure stability, whereas high reduced temperatures oppose it.

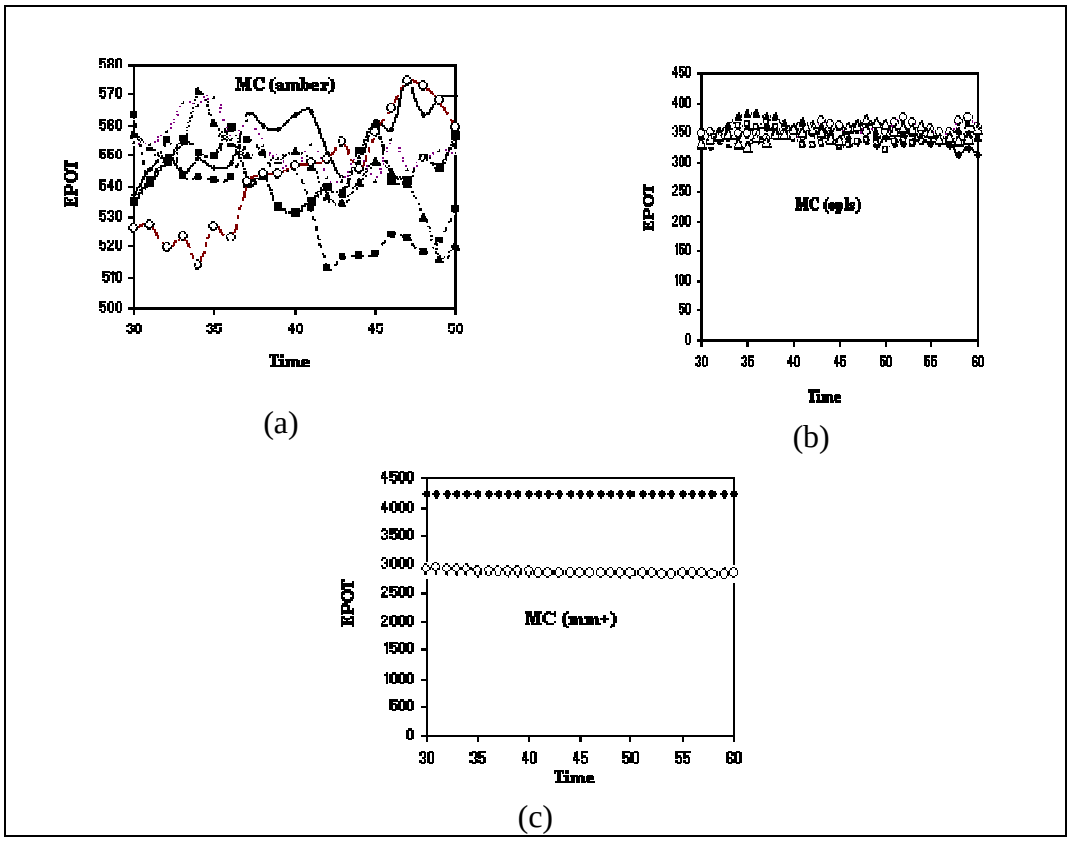

Figure 4: The potential energy(kcal/mol) via time (ps) during Monte Carlo (MC) simulation at 295, 297, 299, 301, 303 and 305 K using **(a)** AMBER **(b)** OPLS and **(c)** MM+ force fields corresponding to a stabilized structure of IGF-1 .

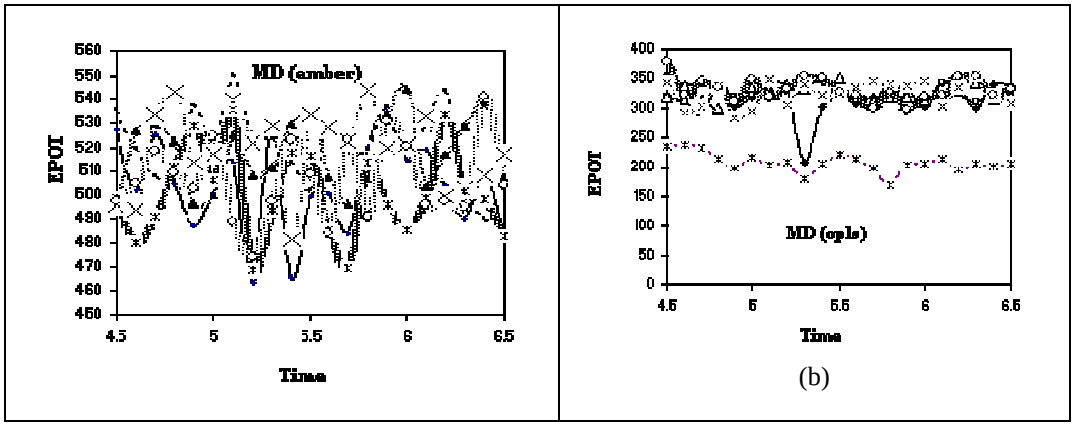

(a)

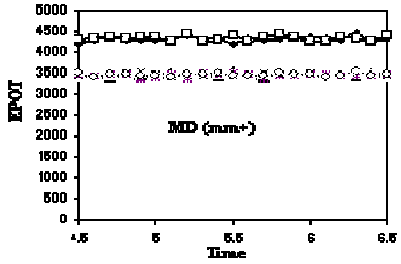

(c)

Figure 5: The potential energy(kcal/mol) via time (ps) during Molecular Dynamic (MD) simulation at 295, 297, 299, 301, 303 and 305 K using **(a)** AMBER (**b)** OPLS and **(c)** MM+ force fields corresponding to a stabilized structure of IGF-1 .

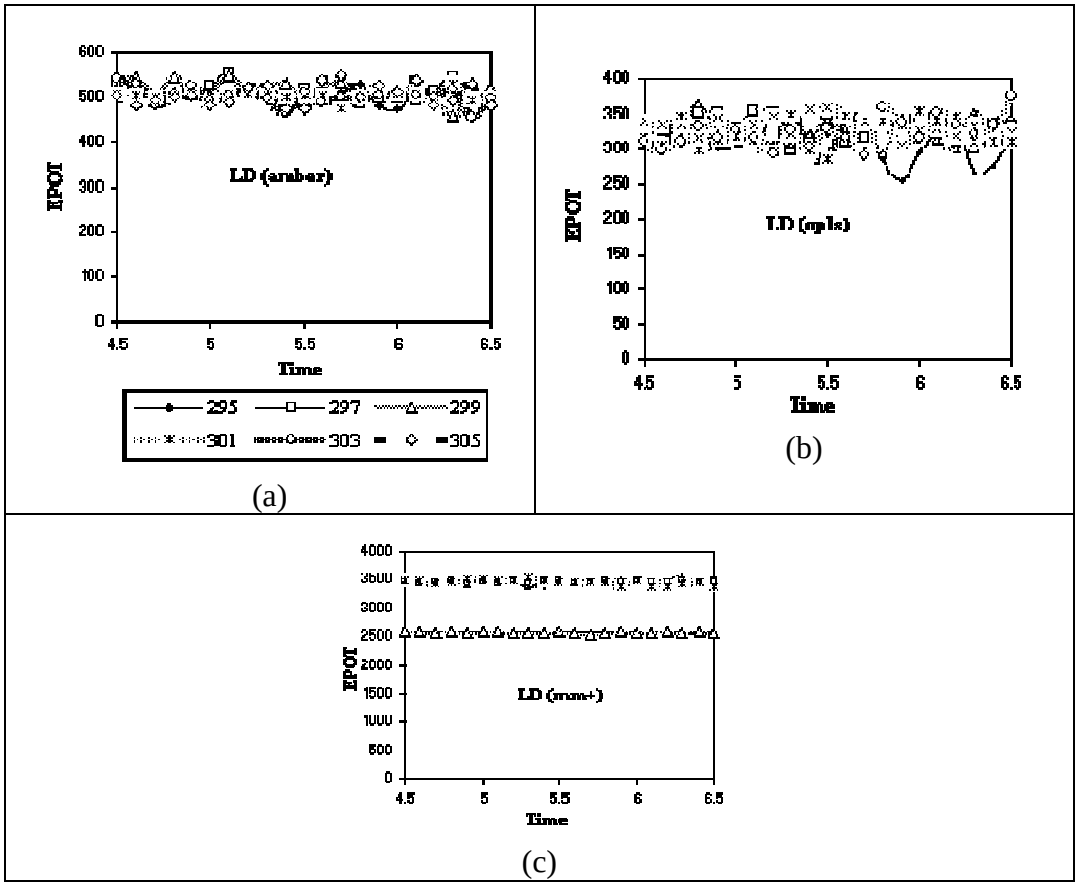

Figure 6: potential energy(kcal/mol) via time (ps) during Langevin Dynamic (LD) simulation at 295, 297, 299, 301, 303 and 305 K using **(a)** AMBER (**b)** OPLS and **(c)** MM+ force fields corresponding to a stabilized structure of IGF-1.

Table 2: Calculated Energy potential (kCal/mol) in various Temperatures for IGF-1 at MM+, AMBER and OPLS.

T(K)		EPOT(MC)					
		MM+		AMBER		OPLS	
295	297	4235.984	2888.215	537.0323	563.3023	354.1178	328.5373
299	301	2906.046	2900.473	557.4321	535.0936	345.7581	343.7589
303	305	2908.884	2917.52	554.7775	526.3257	347.554	331.7875
295	297	4235.91	2883.358	545.3885	542.0403	350.5241	320.7311
299	301	2887.079	2885.448	553.002	541.189	354.173	349.8519
303	305	2900.525	2923.604	554.0753	527.549	351.5697	340.6064
295	297	4235.836	2871.213	550.2813	555.388	345.1127	331.0986
299	301	2873.877	2883.255	549.6397	547.9619	352.4398	343.5526
303	305	2889.936	2912.401	558.5192	519.8594	344.3478	345.3649
295	297	4235.662	2858.414	543.9048	543.5708	345.1661	326.7686
299	301	2869.987	2880.593	554.9779	555.7316	362.0574	350.8972
303	305	2888.042	2902.244	567.5231	523.7003	342.4099	347.168
295	297	4235.785	2864.459	549.2016	542.6379	346.0615	333.429
299	301	2879.702	2870.632	571.1646	551.1309	377.0245	361.2684
303	305	2868.186	2899.195	566.4869	513.8336	347.6069	330.4477
295	297	4235.928	2860.041	545.8426	541.5521	355.5735	331.6525
299	301	2867.552	2873.999	560.8979	549.9072	383.4842	363.6535
303	305	2860.671	2886.921	569.0027	526.6578	348.5785	326.4272
295	297	4235.977	2838.857	547.4008	542.6965	354.9743	334.1456
299	301	2856.91	2850.952	554.6624	559.3318	382.8443	358.8365
303	305	2863.217	2878.897	555.89	523.1423	347.6105	341.3449
295	297	4236.079	2847.769	563.6295	555.1603	358.1401	326.2686
299	301	2841.119	2853.838	549.9271	540.7308	378.2664	366.259
303	305	2865.166	2867.208	561.7354	541.0972	340.2723	334.8615
295	297	4235.939	2841.011	559.6968	550.5739	350.0228	341.2642

T(K)		EPOT(MC)					
		MM+		AMBER		OPLS	
299	301	2854.111	2854.219	551.3961	543.2766	376.6521	359.0934
303	305	2851.653	2869.821	553.7677	543.8042	346.1711	347.44
295	297	4235.915	2840.159	558.8617	543.8674	348.7244	342.525
299	301	2864.091	2847.136	548.6024	533.6068	366.5257	355.267
303	305	2857.226	2870.121	549.1909	544.1115	348.4853	346.989
295	297	4235.679	2850.142	563.642	544.8266	357.2484	339.673
299	301	2859.588	2843.769	551.4084	531.3312	359.5042	345.7718
303	305	2854.746	2866.983	545.3275	546.4106	340.9888	354.5321
295	297	4235.633	2844.473	564.7132	533.1169	363.6589	339.187
299	301	2853.499	2840.504	546.4174	535.2596	369.4149	327.8606
303	305	2848.781	2860.427	554.335	547.3047	343.462	350.2364
295	297	4235.695	2835.124	550.9998	512.8999	360.4237	345.0831
299	301	2842.188	2833.22	536.8683	539.688	363.5614	329.5917
303	305	2841.851	2857.681	542.8929	548.7379	359.5547	354.4125
295	297	4235.842	2834.423	542.9478	516.5182	352.2798	337.6797
299	301	2847.525	2822.857	534.5339	537.8507	360.5002	332.4513
303	305	2839.497	2856.229	541.7733	554.9586	368.2707	349.5836
295	297	4235.807	2842.41	548.394	517.0762	348.838	342.7613
299	301	2852.654	2818.777	541.3942	551.8688	350.7536	339.3084
303	305	2845.101	2859.85	549.7361	545.2499	363.6275	340.7894
295	297	4235.856	2828.16	561.4	517.4912	339.2717	339.9656
299	301	2846.003	2823.927	547.8884	559.1285	359.7528	326.1819
303	305	2846.762	2846.006	541.671	557.965	359.8163	337.309
295	297	4235.738	2813.885	558.9424	524.2564	339.6264	340.827
299	301	2846.063	2826.407	544.5283	541.882	354.9368	329.647
303	305	2835.018	2859.977	555.5255	565.3812	352.9486	358.4168

T(K)		EPOT(MC)					
		MM+		AMBER		OPLS	
295	297	4235.683	2820.807	574.8336	523.1565	333.9953	335.1254
299	301	2848.388	2827.333	540.8102	542.011	365.9344	333.2373
303	305	2837.379	2853.203	545.1721	574.3134	354.3969	360.9447
295	297	4235.73	2828.653	563.7302	517.9006	335.5606	330.472
299	301	2851.181	2836.091	529.7856	549.5345	360.0608	338.0183
303	305	2842.026	2848.864	548.3592	572.5765	350.7377	370.9806
295	297	4235.575	2819.025	569.4018	522.2225	329.4926	326.7581
299	301	2828.133	2830.444	516.1687	546.084	347.6144	330.1531
303	305	2820.963	2838.694	552.3593	568.3253	360.2547	367.6311
295	297	4235.474	2810.148	569.616	532.5905	341.4251	323.0252
299	301	2824.638	2821.123	520.2739	557.0218	345.387	320.7092
303	305	2809.159	2837.105	550.9778	559.1342	350.4919	363.2806

T(K)		EPOT(MD)					
		MM+		AMBER		OPLS	
295	297	4210.79	4288.985	527.3578	535.2763	354.2476	318.2481
299	301	3419.356	3440.532	494.5307	495.9955	319.1986	341.9576
303	305	3455.45	3483.999	498.6193	497.0406	233.3117	377.6465
295	297	4290.329	4320.816	502.2061	519.6428	339.9279	310.6455
299	301	3434.814	3439.83	526.4235	493.8266	336.4753	291.9342
303	305	3443.293	3416.052	480.1488	504.6467	236.4355	320.6327
295	297	4371.666	4350.692	525.0994	507.8335	341.3153	288.8688
299	301	3386.889	3478.571	529.2417	533.0989	312.8945	301.8429
303	305	3460.487	3472.971	490.9563	517.9937	231.1382	344.6291
295	297	4296.785	4329.588	504.7312	505.6049	336.4077	341.1394
299	301	3479.096	3495.251	522.251	542.6166	299.5432	336.3144

T(K)		EPOT(MD)					
		MM+		AMBER		OPLS	
303	305	3462.17	3476.277	511.3409	509.614	213.2367	333.0184
295	297	4303.447	4371.86	487.4169	537.4854	302.3023	317.8343
299	301	3489.193	3518.701	496.4862	513.6497	313.907	281.5862
303	305	3371.318	3426.49	528.2641	502.7837	198.5066	310.0454
295	297	4300.576	4355.381	500.8381	516.929	319.1307	320.479
299	301	3505.641	3453.456	499.9372	516.7252	334.0543	294.9457
303	305	3409.008	3444.407	506.0706	524.8028	214.6883	347.8624
295	297	4309.237	4265.458	513.5359	550.3824	345.2705	332.0029
299	301	3514.08	3402.411	525.3257	539.2837	322.789	347.5192
303	305	3466.064	3413.669	535.2093	489.278	203.4976	319.6483
295	297	4401.925	4443.53	463.4955	524.0253	330.9887	307.1991
299	301	3421.173	3422.556	508.1931	522.0677	340.3782	304.4567
303	305	3370.795	3468.461	468.5343	473.9662	208.2185	330.4919
295	297	4284.895	4278.622	527.4733	523.5819	208.2185	330.4919
299	301	3415.884	3449.611	511.243	528.6366	331.4785	338.7397
303	305	3484.139	3482.982	493.9665	497.0681	178.9832	351.4939
295	297	4345.033	4310.343	465.7351	514.3511	301.7872	348.601
299	301	3421.798	3485.754	529.0999	481.7465	324.3557	322.1682
303	305	3461.478	3515.989	517.4446	522.877	204.1998	349.8143
295	297	4215.188	4384.653	499.0536	501.712	317.7411	325.0367
299	301	3530.324	3437.044	533.8555	533.4912	349.8931	324.2932
303	305	3507.608	3431.513	516.1681	508.7436	219.8929	325.5009
295	297	4330.001	4281.668	500.4392	531.2556	307.7915	311.8912
299	301	3462.701	3451.626	507.1952	527.718	333.3354	334.4424
303	305	3454.264	3422.529	485.2639	484.4238	213.4292	321.2014
295	297	4303.186	4365.847	483.8532	518.2829	318.0182	306.6712
299	301	3394.981	3489.914	496.1218	522.541	310.7109	345.0437

T(K)		EPOT(MD)					
		MM+		AMBER		OPLS	
303	305	3377.382	3447.376	469.0301	522.9171	197.4162	299.3484
295	297	4326.629	4445.121	520.0923	518.8304	319.1497	344.6331
299	301	3514.473	3476.453	506.4193	543.2968	318.6115	339.1389
303	305	3447.624	3484.363	513.571	491.1841	169.4245	326.2012
295	297	4366.921	4358.478	534.6727	537.1	331.8006	324.4326
299	301	3467.887	3434.047	533.4216	519.5013	318.7386	337.4207
303	305	3418.719	3461.921	495.7306	530.857	201.4282	296.0907
295	297	4358.029	4280.032	515.1163	520.4341	301.7409	311.0852
299	301	3453.021	3500.615	544.1592	520.9449	313.7343	343.6175
303	305	3476.481	3478.572	485.7271	520.3431	205.9013	319.3591
295	297	4341.226	4272.062	519.3115	529.032	342.0903	342.3374
299	301	3469.677	3453.05	503.5554	532.517	320.2513	302.2707
303	305	3474.609	3393.49	498.4059	495.9245	213.9004	321.8973
295	297	4302.709	4355.351	503.8653	543.6403	337.7553	324.653
299	301	3460.494	3440.337	516.6548	499.4484	338.2431	334.1742
303	305	3425.421	3445.563	533.1451	497.0183	195.717	353.9156
295	297	4452.299	4335.674	490.5256	501.5159	299.9477	311.4561
299	301	3417.058	3488.196	528.3224	502.3401	342.9102	355.2545
303	305	3449.055	3537.28	501.5012	495.1578	205.6	353.6971
295	297	3449.055	3537.28	509.4262	490.1977	338.5802	328.9518
299	301	3496.024	3448.752	538.645	507.7447	315.2097	322.3077
303	305	3449.451	3443.293	497.5652	540.6433	201.1053	319.8668
295	297	4328.744	4388.186	484.329	487.0341	338.1252	320.3201
299	301	3508.281	3437.637	507.1878	516.707	318.6565	307.1662
303	305	3455.588	3481.294	482.9492	503.6921	206.5169	330.3023

T(K)	EPOT(LD)

		MM+		AMBER		OPLS	
295	297	2579.846	3405.258	513.2186	528.15	321.3818	311.2994
299	301	2569.473	3506.185	518.6368	508.0626	343.8734	339.2246
303	305	3480.613	3450.559	539.5172	502.6813	316.3417	311.1847
295	297	2589.535	3444.03	499.7869	516.0245	322.7999	308.6239
299	301	2578.557	3467.769	543.1108	501.8044	326.8775	332.2738
303	305	3495.918	3421.9	530.5234	482.4206	305.1587	298.222
295	297	2567.801	3432.501	508.1079	497.8874	322.6342	343.9134
299	301	2546.555	3458.191	502.9492	500.4421	339.418	332.5635
303	305	3428.675	3470.391	479.7136	493.0887	346.9156	310.3809
295	297	2588.488	3409.925	512.786	496.3951	328.6388	351.7402
299	301	2568.802	3477.177	544.3472	502.4798	363.9548	315.3748
303	305	3455.711	3486.662	507.2958	500.5871	296.7043	329.4997
295	297	2590.098	3408.431	505.4064	508.2617	301.2283	351.383
299	301	2552.44	3465.14	505.245	521.7915	320.9432	343.0555
303	305	3507.042	3430.872	525.1266	502.9998	311.7542	315.791
295	297	2577.903	3472.735	482.6723	524.14	304.7759	328.6955
299	301	2577.913	3479.335	503.0349	489.6058	323.2028	322.9286
303	305	3503.99	3469.163	492.9588	479.1641	317.0148	326.6403
295	297	2585.024	3409.999	501.673	551.8837	305.6494	353.8895
299	301	2573.96	3472.471	548.2233	507.2563	333.6927	333.4404
303	305	3472.611	3439.305	501.8165	489.4213	313.1117	316.1416
295	297	2563.826	3454.12	524.3984	503.3033	341.5131	350.8395
299	301	2565.485	3459.745	506.735	507.7916	305.9	345.6635
303	305	3474.678	3488.03	514.5964	520.7366	294.8215	293.1924
295	297	2569.188	3385.981	490.5222	519.7032	324.46	297.4873
299	301	2564.208	3433.359	525.5302	504.838	305.8051	320.024
303	305	3541.201	3426.485	495.4621	527.0049	349.1488	325.338
295	297	2559.526	3414.71	489.266	505.9484	314.4352	313.0575

T(K)		EPOT(LD)					
		MM+		AMBER		OPLS	
299	301	2566.563	3401.513	529.5195	500.1281	321.0137	356.852
303	305	3476.94	3474.156	467.2895	473.4712	297.3159	301.3034
295	297	2584.529	3460.82	516.8234	517.6833	319.8571	346.1244
299	301	2569.737	3443.905	490.1534	502.6556	337.8195	358.6917
303	305	3448.999	3474.151	512.2114	473.2974	285.3812	328.9042
295	297	2574.05	3398.087	492.1332	511.4382	345.2494	311.3421
299	301	2561.146	3397.049	511.8376	504.886	328.7564	346.241
303	305	3448.117	3429.749	489.7065	538.1508	346.3618	314.3207
295	297	2571.361	3429.874	510.5202	482.568	342.7836	316.2462
299	301	2531.758	3435.588	531.8323	474.8859	338.4859	297.9369
303	305	3463.164	3457.529	500.7173	546.606	338.8057	290.12
295	297	2569.537	3467.652	527.666	484.2487	285.2081	339.9539
299	301	2562.692	3396.74	500.7725	499.8272	292.3938	340.2541
303	305	3448.279	3472.96	494.8175	498.7156	337.9184	359.5291
295	297	2569.649	3450.92	482.1576	514.1124	253.1677	332.026
299	301	2573.344	3493.333	499.376	516.9822	342.8565	304.5523
303	305	3371.327	3464.815	504.6794	524.4158	332.0623	336.4991
295	297	2570.01	3453.387	472.2345	495.7901	294.4622	326.0108
299	301	2552.84	3438.135	513.3206	506.941	328.7103	324.6017
303	305	3472.448	3493.887	512.1343	510.7655	354.5991	314.9204
295	297	2555.729	3441.786	516.4899	492.0165	325.7104	320.921
299	301	2564.157	3449.956	523.1369	507.9351	312.8271	328.0562
303	305	3387.85	3468.916	503.0721	538.5077	337.9524	350.9694
295	297	2571.258	3404.964	505.9321	515.333	335.3871	309.2835
299	301	2571.988	3465.41	498.7625	485.5512	299.1711	319.1378
303	305	3392.038	3458.916	499.8112	482.5093	345.6826	332.3725
295	297	2562.191	3446.998	522.1642	542.3101	265.5349	299.0892

T(K)		EPOT(LD)					
		MM+		AMBER		OPLS	
299	301	2563.942	3523.837	459.5745	528.3569	353.7659	329.5145
303	305	3438.471	3486.51	519.3807	493.3634	310.4973	320.9409
295	297	2573.969	3433.049	488.3241	487.7672	276.904	335.0679
299	301	2570.754	3442.332	489.7299	491.5191	312.0651	310.3455
303	305	3459.938	3453.697	455.7375	528.3239	309.7843	332.9762
295	297	2573.179	3486.304	503.837	492.3624	316.411	330.6078
299	301	2562.767	3451.816	518.1656	496.1881	342.388	322.0578
303	305	3392.909	3466.878	497.1192	480.7999	310.8878	374.3974

These results have also revealed that the solvation of IGF-1 is the major component for the interaction potential energy and it was clearly shown that the role of the solute-solvent interactions is more pronounced in IGF-1 solvation. The major part of this difference is due to the interaction of IGF-1 with solvent molecules that corresponds to various simulation methods and force fields. A difficult task in computational study of stabilized structure is to find a proper energy function that can lead to a unique structure. Our simulations showed that the simple energy function modified to include solvent effect has a parameter range that can simulate indicated structure at a constant temperature of 300 K.

CONCLUSION

In this study we have used molecular dynamic models to explore the stability of IGF-1 by comparing theoretical methods of simulation. A highly selective effect of temperature and environment was discovered in the chemical structure and it has been investigated at a standard constant temperature with MC, MD and LD simulations. We have employed the molecular dynamics simulation method as the main tool to study conformational dynamics of biomolecules.

One of the force field designed for treating macromolecules can be simplified by not considering explicitly – the so-called united atom approach is AMBER. It appears that solvent effects influence the calculated potential energy surface, by lowering potential energy barriers on angle. This means that the parameterizations that have been developed for small molecules with considerable effort can be carried over into macromolecular calculations with little or no change.

Also, we have applied the MM+ and OPLS force fields parameters for IGF-1 model in gas and for water environments. Also, the possible difference between the IGF-1 intramolecular VDW attraction and that with water has been included in the hydrophobic interaction energy. The short- range repulsion represents the exclusive volume of each atom and needs to be calculated explicitly.

The measurement of the potential of solvation under similar conditions of temperature in solution along with

investigation of energetic and structural aspects of solution have been used to gain insight into the molecular level interaction with IGF-1. Solute–solvent pair interaction of potential energies has shown that the greater stability of solvent observed over all states investigated in this study is related to the MD/AMBER approach.

REFERENCES

Berendsen WF 1990 Computer simulation of molecular dynamics methodology, applications, and perspectives in chemistry. *Angew. Chem.* **29**: 992-1023.

Chandler D, Weeks JD and Andersen HC, Van der Waals picture of liquids, solids, and phase transformations, *Science*. **220**: 787-794.

Cornell WD, Cieplak P, Bayly CI, Gould IR, Merz KM, Ferguson DM, Spellmeyer DC, Fox T, Caldwell JW and Kollman PA 1995 A second generation force field for the simulation of proteins, nucleic acids, and organic molecules. *J. Am. Chem. Soc*. **117**: 5179-5197.

Daura X, Jaun B, Seebach D, van Gunsteren WF and Mark AE, 1998 Reversible peptide folding in solution by molecular dynamics simulation. *J. Mol. Biol*. **280**: 925–932.

Dzubiell J, Swanson JMJ and McCammon JA 2006 Coupling Hydrophobicity, Dispersion, and Electrostatics in Continuum Solvent Models. *Phys. Rev. Lett.* **96**: 087802 1-4 .

Emmitte KA, Wilson BJ, Baum EW, Emerson HK, Kuntz KW, Nailor KE, Salovich JM, Smith SC, Cheung M, Gerding RM, Stevens KL, Uehling DE, MookJr RA, Moorthy GS, Dickerson SH, Hassell AM, Leesnitzer MA, Shewchuk LM, Groy A, Rowand JL, Anderson K, Atkins CL, Yang J, Sabbatini P, Kumar R 2009 Discovery and optimization of imidazo[1,2-a]pyridine inhibitors of insulin-like growth factor-1 receptor (IGF-1R). *Bioorg. Med. Chem. Lett.* **19**: 1004-1008.

Hagler AT and Lifson S 1974 Energy functions for peptides and proteins. II. Amide hydrogen bond and calculation of amide crystal properties. *J. Am. Chem. Soc*. **96**: 5327-5335.

Hamaneh MB and Buck M 2007 Acceptable Protein and Solvent Behavior in Primary Hydration Shell Simulations of Hen Lysozyme. *Biophys J*. **92**: 7, 49-51.

Hermida-Ramón JM, Öhrn A and Karlström G 2009 Aqueous solvent effects on structure and lowest electronic transition of methylene peroxide in an explicit solvent model. *Chem. Phys.* **359**: 118–125.

HyperChem 7.0 2001 Hypecube Inc., Gainesville, FL, USA.

Jorgensen WL and Tirado-Rives J 1988 The OPLS potential functions for proteins: Energy minimizations for crystals of cyclic peptides and crambin. *J. Am. Chem. Soc*. **110**: 1657-1666.

Jorgensen WL, Maxwell DS and Tirado-Rives J 1996 Development and testing of the OPLS all atom force field on conformational energetics and properties of organic liquids, *J. Am. Chem. Soc.* **118**: 11225–11236.

Karplus M and Petsko GA 1990 Molecular dynamics simulations in biology. *Nature*. **347**: 631- 639.

Kitchen DB, Decornez H, Furr JR, and Bajorath J 2004 Docking and Scoring in Virtual Screening for Dryug Discovery: Methods and Applications. *Nature*. **3**: 935-949.

Laajok LG, Francis GL, Wallace JC, Carver JA and Keniry MA 2000 Solution Structure and Backbone Dynamics of Long-[Arg^3]insulin-like Growth Factor-I. *J. Biol. Chem*. **275**: 10009-10015.

Li Y, Higashi Y, Itabe H, Song YH, Du J and Delafontaine P 2003 Insulin-like growth factor-1 receptor activation inhibits oxidized LDL-induced cytochrome-c release and apoptosis via the phosphatidylinositol 3 kinase/Akt

signaling pathway, Arterioscler. *Thromb. Vasc. Biol.* **23**: 2178-2184.

McCammon JA, Northrup SH, Karplus M, and Levy RM 1980 Helix-coil transitions in a simple polypeptide model, Biopolymers. **19** 2033-2045.MacKerell Jr AD, Bashford D, Bellott M, Dunbrack, Jr RL, Evanseck JD, Field MJ, Fischer S, Gao J, Guo H, Ha S, Joseph-McCarthy D, Kuchnir L, Kuczera K, Lau FTK, Mattos C, Michnick S, Ngo T, Nguyen DT, Prodhom B, Reiher WE, Roux B, Schlenkrich M, Smith JC, Stote R, Straub J, Watanabe M, Wio´rkiewicz-Kuczera J, Yin D, and Karplus M 1998 All-atom empirical potential for molecular modeling and dynamics studies of proteins. *J. Phys. Chem. B* **102**: 3586-3616.

McGuire RF, Momany FA and Scheraga HA 1972 Energy parameters in polypeptides. V. Empirical hydrogen bond potential function based on molecular orbital calculations. *J. Phys. Chem.* **76**: 375-393.

Náray-Szabó G, and Berenteb I 2003 Computer modeling of enzyme reactions, *J. Mol. Struct.* **666**: 637-644.

Ozkan SB, Dalgy´n GS and Haliloglu T 2004 Unfolding events of Chymotrypsin Inhibitor 2 (CI2) revealed by Monte Carlo (MC) simulations and their consistency from structure-based analysis of conformations. *Polymer.* **45**: 581–595.

Phillips JC, Braun R, Wang W, Gumbart J, Tajkhorshid E, Villa E, Chipot C, Skeel RD, Kalé L and Schulten K 2005 Scalable Molecular Dynamics with NAMD. J. *Comput. Chem.* **26**: 1781-1802.

Ponder JW and Case DA 2003 Force fields for protein simulations. *Adv. Protein Chem*. **66**: 27- 85.

Sung S and Wu XW 1997 Molecular dynamics simulations of helix folding: the effects of amino acid substitution. *Biopolymers*. **42**: 633-644.

Sung SS, 1999 Monte Carlo Simulations of β-Hairpin Folding at Constant Temperature. *Biophys. J.* **76**: 164 -175.

Tafazzoli M and Khanlarkhani A 2007 Theoretical investigation of the enhanced solubility of perfluorobenzene in the supercritical carbon dioxide as a function of temperature and density by Monte Carlo simulation. *Chem. Phys. Lett.* **444**: 48–55.

Weiner SJ,. Kollman PA, Case DA, Singh UC, Ghio C, Alagona G, Profeta S and Weiner P 1984 A new force field for molecular mechanical simulation of nucleic acids and proteins, *J. Am. Chem. Soc.* **106**: 765–784.